Stability enhancement of a Single Machine Infinite Bus system using H-infinity control

Abdeslem Khelloufi, Bilal Sari
DAC Laboratory, Department of Electrical Engineering
University of Setif 1
Setif, Algeria
abdeslem.khelloufi@univ-setif.dz
bilal.sari@univ-setif.dz

Seif Eddine Chouaba
DAC Laboratory
University of Setif 1
Setif, Algeria
seif.chouaba@univ-setif.dz

***Abstract*—This work presents a robust H_∞ output feedback control design of a Power System Stabilizer (PSS). This PSS is used to damp low-frequency oscillations in power systems over a wide range of operating conditions. The H_∞ control is employed in the Single-Machine connected to an Infinite Bus (SMIB) system using two weighting functions. The proposed stabilizer offers robust stability against different external disturbances and parameter uncertainties. A comparative simulation study shows a significantly enhancement and good performance of the proposed design compared to an IEEE conventional power system stabilizer.**

***Index Terms*—SMIB, Power System Stabilizer, H_∞ synthesis, Robust Control**

I. Introduction

The low-frequency oscillations are a challenge in the stability of power systems, which can lead to blackouts. These oscillations are divided into an inter-area mode, a torsional mode, and a local mode. Among the controllers used to damp low-frequency oscillations is power system stabilizers (PSS), which used to generate a supplementary damping torque signal through the excitation system [1], [2].

The conventional power system stabilizers are based on a lead-lag compensator. In the current IEEE standard [3], The types of power system stabilizers according to the number of inputs are classified in two categories: single-input like (PSS1A, PSS5C) and dual-input like (PSS2C, PSS3C, PSS4C, PSS6C, PSS7C). According to the working frequency bands,there are two types: single frequency band like (PSS1A, PSS2C,...), and multiple frequency bands like (PSS4C, PSS5C) which used to damp separate frequency bands (very low, low, intermediate, and high-frequency modes) [3]. In the literature, numerous methods have been developed to damp low-frequency oscillations. The sliding mode control (SMC) is presented in paper [4], pole placement techniques in [5], a farmland fertility algorithm (FFA) [6], a genetic algorithm [7], a Particle Swarm Optimization (PSO) [8], Bio-inspired Algorithms [9]. Therefore, artificial intelligence-based training and tuning techniques have been used to develop a PSS as a Deep Reinforcement Learning-Based method [10], adaptive neural networks approach [11], a fuzzy logic controller [12]. Furthermore, robust control theories have been employed in the design of robust power system stabilizers [13]. At the nominal operating conditions, the conventional power system stabilizer (CPSS) works efficiently, but its performance decreases if the operating point has changed [14]. In this case, the CPSS does not guarantee the power system robustness for different range of operating points. To solve the robustness problem, the robust control design guarantees stability under external disturbance or parametric uncertainties. In [15], the authors have been designed their PSS using the concept of Glover-McFarlane's loop shaping design. A Linear Matrix Inequalities (LMI) technique is used to synthesize a robust PSS usnig pole-placement [16]. Robust control methods based on H_2 and H_∞ Norm designed in [14] have been applied on an SMIB using three weighting functions. In this work, an H_∞ control approach has been developed on the SMIB using two weighting functions. This paper is organized as follows. Section II presents the description and mathematical model of the SMIB. Section III gives the control problem formulation. Section IV explains the proposed resolution and chosen weighting functions in the proposed design. Section V shows simulation results, in which a comparative study is performed between the proposed control strategy and the conventional CPSS. Finally, Section VI ends this paper and gives some concluding observations.

II. Plant Model

A SMIB system consists of a Single Machine connected to Infinite Bus through an external reactance X_e and an external resistance R_e, as shown in Fig.1.

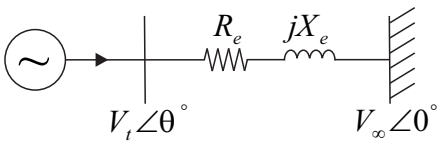

Fig. 1. Diagram of SMIB system.

The mathematical model of the synchronous machine is described by the equations given below [1]:

$$\dot{\omega} = \frac{\omega_s}{2H}[T_m - (E_q^{'} I_q + (X_q - X_d^{'}) I_d I_q) - D(\omega - \omega_s)] \quad (1)$$

$$\dot{\delta} = (\omega - \omega_s) \quad (2)$$

$$\dot{E}_q^{'} = \frac{1}{T_{do}^{'}}[E_q^{'} + (X_d - X_d^{'})I_d - E_{fd}] \quad (3)$$

$$\dot{E}_{fd}^{'} = \frac{1}{T_A}[-E_{fd} + K_A(V_{ref} - V_t)] \quad (4)$$

Where all the notations are given in the appendix.
The Heffron-Philips model scheme of the SMIB system is shown in Fig.2.

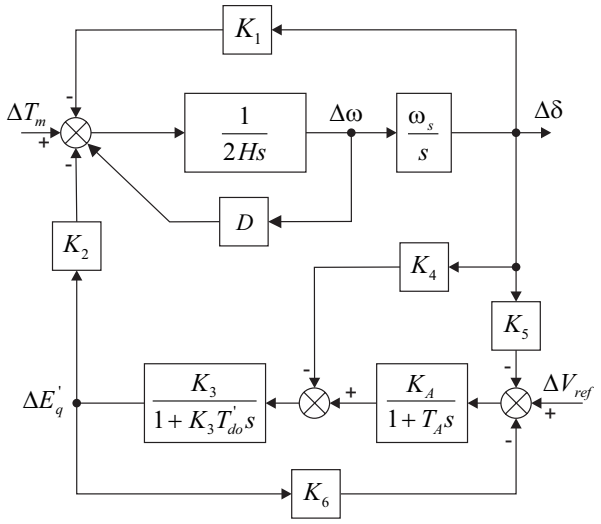

Fig. 2. Scheme of Heffron-Phillips model.

The linearized state-space model will be considered [17]:

$$\begin{aligned} \Delta\dot{x}(t) &= A\Delta x(t) + B_1\Delta w(t) + B_2\Delta u(t) \\ \Delta y(t) &= C\Delta x(t) \end{aligned} \quad (5)$$

The matrices A,B and C are defined as:

$$A = \begin{bmatrix} \frac{-1}{K_3T_{do}^{'}} & \frac{-K_4}{T_{do}^{'}} & 0 & \frac{1}{T_{do}^{'}} \\ 0 & 0 & \omega_s & 0 \\ \frac{-K_2}{2H} & \frac{-K_1}{2H} & \frac{-D\omega_s}{2H} & 0 \\ \frac{-K_AK_6}{T_A} & \frac{-K_AK_5}{T_A} & 0 & \frac{-1}{T_A} \end{bmatrix} \quad (6)$$

$$B = [B_1|B_2] = \begin{bmatrix} 0 & 0 & 0 \\ 0 & 0 & 0 \\ 0 & \frac{1}{2H} & 0 \\ \frac{K_A}{T_A} & 0 & \frac{K_A}{T_A} \end{bmatrix}, \quad (7)$$

$$C = \begin{bmatrix} 0 & 0 & 1 & 0 \end{bmatrix}, \quad (8)$$

where $\Delta x(t) = \begin{bmatrix} \Delta E_q^{'} & \Delta\delta & \Delta v & \Delta E_{fd} \end{bmatrix}^T$ is the state vector, $\Delta w(t) = \begin{bmatrix} \Delta V_{ref} & \Delta T_m \end{bmatrix}^T$ is a vector of the external inputs (External disturbances), the control signal of the power system stabilizer $\Delta u(t) = \Delta V_{pss}$ and the system output signal is $\Delta y = \Delta v$. The SMIB system data and the relationships of the model's K-constants are given in the appendices

III. Control Problem Formulation

The general configuration of the problem is illustrated in the Fig.3, where the augmented plant transfer matrix is $P(s)$, the robust controller is $K(s)$, the external inputs w are the reference voltage variation ΔV_{ref} and the mechanical torque variation ΔT_m, the measurement output y is the speed deviation, the control signal u is the output of H_∞ Power System Stabilizer (HPSS) and the external outputs z will be given in the next section.

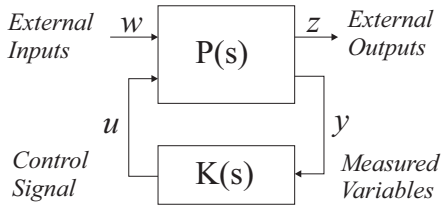

Fig. 3. Standard control configuration.

The open-loop transfer matrix from $\begin{bmatrix} z \\ y \end{bmatrix}$ to $\begin{bmatrix} w \\ u \end{bmatrix}$ is given as follows:

$$\begin{bmatrix} z \\ y \end{bmatrix} = \begin{bmatrix} P_{11}(s) & P_{12}(s) \\ P_{21}(s) & P_{22}(s), \end{bmatrix} \begin{bmatrix} w \\ u \end{bmatrix} \quad (9)$$

The linear Fractional Transformation (LFT) representation of the system in closed loop is given as follows:

$$T_{zw}(s) = P_{11}(s) + P_{12}(s)K(s)[I - P_{22}(s)K(s)]^{-1}P_{21}(s) \quad (10)$$

The H_∞ control problem is formulated as the minimisation of the H_∞ norm γ of the closed loop transfer matrix as follows:

$$||T_{zw}(s)||_\infty < \gamma \quad (11)$$

The state space representation of the standard problem configuration is given by the following form:

$$\begin{bmatrix} \dot{x} \\ z \\ y \end{bmatrix} = \begin{bmatrix} A & B_1 & B_2 \\ C_1 & D_{11} & D_{12} \\ C_2 & D_{21} & D_{22} \end{bmatrix} \begin{bmatrix} x \\ w \\ u \end{bmatrix} \quad (12)$$

where

$$B_1 = \begin{bmatrix} 0 & 0 \\ 0 & 0 \\ 0 & \frac{1}{2H} \\ \frac{K_A}{T_A} & 0 \end{bmatrix}, B_2 = \begin{bmatrix} 0 \\ 0 \\ 0 \\ \frac{K_A}{T_A} \end{bmatrix}, D_{11} = \begin{bmatrix} 1 & 0 \\ 0 & 0 \end{bmatrix},$$

$$C_1 = \begin{bmatrix} -K_6 & -K_5 & 0 & 0 \\ 0 & 0 & 0 & 0 \end{bmatrix}, D_{12} = \begin{bmatrix} 0 \\ 1 \end{bmatrix},$$

$$C_2 = \begin{bmatrix} 0 & 0 & 1 & 0 \end{bmatrix}, D_{21} = \begin{bmatrix} 0 & 0 \end{bmatrix}, D_{22} = \begin{bmatrix} 0 \end{bmatrix},$$

and A is defined in (6). One recalls that all the notations used in this state space model are given in the appendix.

IV. $H\infty$ Controller Resolution

It is necessary to include weighting functions $W_1(s)$ and $W_2(s)$ in the Plant to get some dynamical performances in an H_∞ problem. The Fig.4 illustrates the augmented plant with the weighting functions $W_1(s)$ and $W_2(s)$. The new considered external outputs are: z_1 and z_2, where z_1 is the speed deviation Δv connected to error weighting function W_1 ($z_1 = W_1(s)\Delta v$) and z_2 is the control output u connected to control weighting function W_2 ($z_2 = W_2(s)u$). The choice of these weighting functions is an essential step, an error weighting function W_1 is chosen to limit the speed deviation peak Δv. It is given by the following gain:

$$W_1(s) = \frac{1}{\Delta v_{max}} \tag{13}$$

The control weighting function $W_2(s)$ is used to accelerate the convergence of the HPSS output ΔV_{pss} to zero and therefore, the settling time of the speed deviation will be decreased. The weighting function $W_2(s)$ structure is given by the following equation:

$$W_2(s) = \frac{w_b}{s + w_b \cdot \epsilon} \tag{14}$$

Where w_b and ϵ are the tuning parameters. The following values satisfy the performance requirements for the considered nominal operating point ($P = 0.8p.u., Q = 0.4p.u.$ and $X_e = 0.2p.u.$):
$\Delta v_{max} = 10^{-3}$, $w_b = 62.5$ and $\epsilon = 10^{-4}$.
The resolution of H_∞ problem is carried out by using the LMI toolbox of Matlab. The found gamma is $\gamma = 21.288$. The obtained stabilizer HPSS can be put under the following form:

$$K(s) = \frac{a_1 s^4 + a_2 s^3 + a_3 s^2 + a_4 s + a_5}{b_0 s^5 + b_1 s^4 + b_2 s^3 + b_3 s^2 + b_4 s + b_5} \tag{15}$$

The numerical values of HPSS are given in the next table I:

TABLE I
THE HPSS DATA

Parameter	Value	Parameter	Value
a_1	$-8.72 \cdot 10^{-4}$	b_1	$8.605 \cdot 10^{-11}$
a_2	$-2.37 \cdot 10^{-3}$	b_2	$3.00 \cdot 10^{-7}$
a_3	$2.93 \cdot 10^{-1}$	b_3	$4.39 \cdot 10^{-4}$
a_4	2.94	b_4	$8.53 \cdot 10^{-2}$
a_5	$1.83 \cdot 10^{-2}$	b_5	$2.45 \cdot 10^{-8}$
b_0	$1 \cdot 10^{-14}$		

V. Simulation Results

To verify the effectiveness and the robustness of the proposed HPSS, several studies have been performed on the SMIB system at different operating points where the data of the system are given in the Appendix. Furthermore, a comparative study is carried out with a conventional CPSS. In fact, three different operating points have been considered with respect to the active power P, the reactive power Q, and the reactance of the transmission line X_e. A 5% step disturbance at the AVR voltage reference input is applied for the following tests:

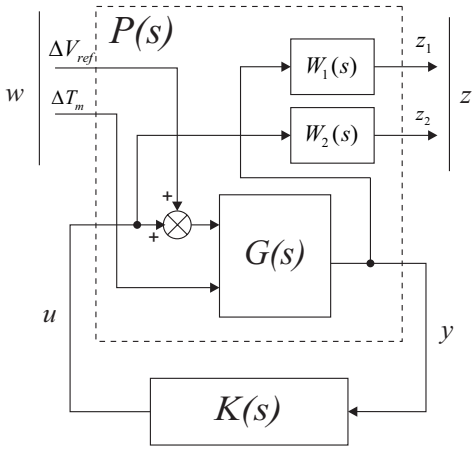

Fig. 4. Weighting functions augmentation of the system.

- 1^{st} Test (T1): $P = 0.8p.u, Q = 0.4p.u$ and $X_e = 0.2p.u.$
- 2^{nd} Test (T2): $P = 0.8p.u, Q = 0.0p.u$ and $X_e = 0.6p.u.$
- 3^{rd} Test (T3): $P = 1.0p.u, Q = 0.5p.u$ and $X_e = 0.7p.u.$

The Fig. 5, Fig. 6 and Fig. 7 present a system response using the conventional PSS (CPSS) and the proposed stabilizer (HPSS) to a 5% step disturbance at the AVR voltage reference input of the three tests (T1, T2 and T3).

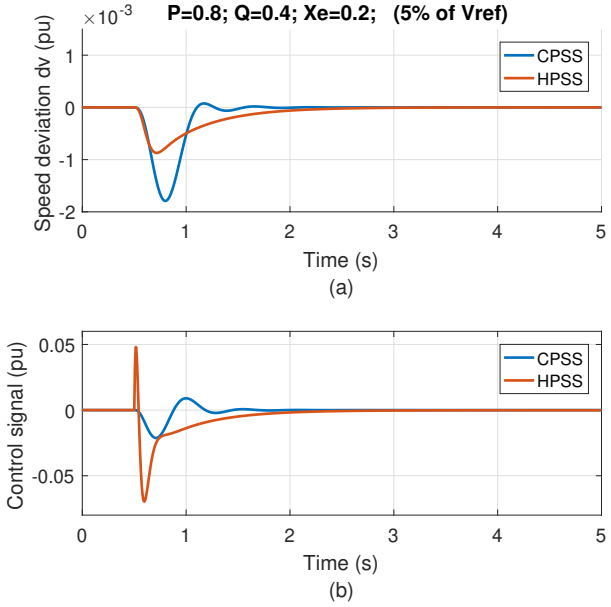

Fig. 5. SMIB response to a 5% step disturbance at the voltage reference input for the test (T1), ($P = 0.8, Q = 0.4$ and $X_e = 0.2$).

Comparing the simulation results obtained with the HPSS with a conventional CPSS shows that the proposed stabilizer achieves good robustness and performances. As can be observed in Fig.5, Fig.6 and Fig.7, the amplitude of the first oscillation of the proposed HPSS is less than the conventional CPSS in all the performed tests (T1, T2 and T3), where the conventional CPSS can not stabilize the system in the 2^{nd}

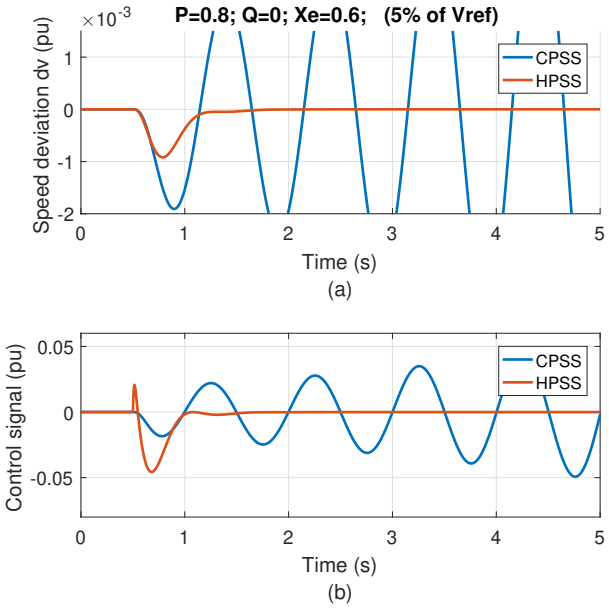

Fig. 6. SMIB response to a 5% step disturbance at the voltage reference input for the test (T2), ($P = 0.8, Q = 0.0$ and $X_e = 0.6$).

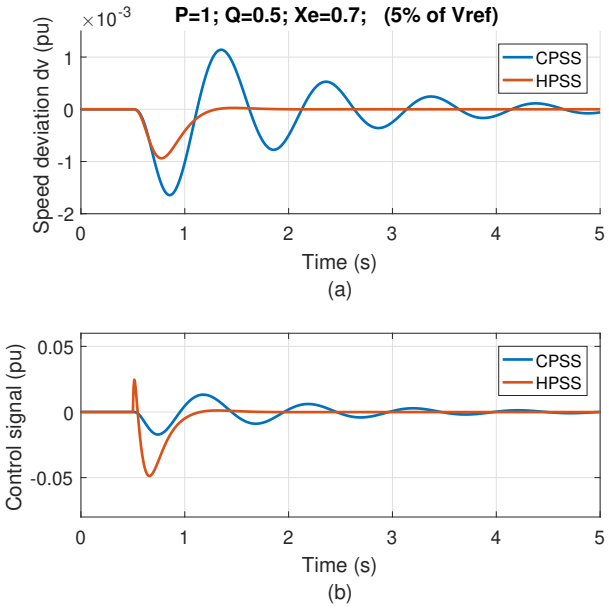

Fig. 7. SMIB response to a 5% step disturbance at the voltage reference input for the test (T3), ($P = 1.0, Q = 0.5$ and $X_e = 0.7$).

test and it has many oscillations in the 3^{rd} test. Moreover, the proposed HPSS has just one oscillation in all the performed tests. The settling times of the proposed HPSS are the least in both the 2^{nd} test and the 3^{rd} test. The control signal of the proposed design is in the range $-0.1 < V_{pss} < 0.1$ in all the tests as recommended by IEEE standard [3] which demonstrates the feasibility of the real implementation. The Table II shows a quantitative comparison of the proposed HPSS with a conventional CPSS. Where, the calculated parameter $\overline{y}_1$ represents the first oscillation amplitude of the system response, $\overline{y}_2$ is the amplitude of the second oscillation and t_s is the settling time for $|y| < 0.0001$. It is noted that the conventional CPSS gives a better settling time only in the first test compared to the proposed HPSS. However, with this CPSS, the stability is not preserved in the second test and the system became too slow in the third test. It is noted that the proposed HPSS has preserved the system stability for all three operating points. Furthermore, it is clear that the proposed HPSS has a better dynamical performance in terms of oscillations damping.

TABLE II
COMPARISON OF PERFORMANCE BETWEEN THE CONVENTIONAL PSS (CPSS) AND THE PROPOSED PSS (HPSS).

		1st Test	2nd Test	3rd Test
1^{st} amplitude $\bar{y}_1$ in p.u.	HPSS	$0.87 \cdot 10^{-3}$	$0.92 \cdot 10^{-3}$	$0.94 \cdot 10^{-3}$
	CPSS	$1.79 \cdot 10^{-3}$	Unstable	$1.64 \cdot 10^{-3}$
2^{nd} amplitude $\bar{y}_2$ in p.u.	HPSS	0.0	0.0	0.0
	CPSS	$0.75 \cdot 10^{-4}$	Unstable	$11.41 \cdot 10^{-4}$
Settling time t_s in s.	HPSS	1.26	0.64	0.67
	CPSS	0.57	Unstable	3.96

VI. CONCLUSION

This paper has presented a robust power system stabilizer design using H_∞ control to enhance the stability and robustness of the Single Machine connected to an Infinite Bus system (SMIB) against an external disturbance (Reference voltage variation ΔV_{ref} or mechanical torque variation ΔT_m). Three different unknown loads with several values of the external impedance X_e (represented by the three considered operating conditions) have been performed. The proposed HPSS controller has a simple architecture, simple weighting functions, good performance and good robustness compared to the conventional CPSS. The simulation results confirm the great benefit of the proposed HPSS compared to the conventional CPSS regarding the stability, the disturbance rejection, the speed deviation dynamical performances.

APPENDIX

A. The SMIB Equations

In this section, the relationships between the system parameters have been defined for a single machine connected to an infinite bus [18]. The values of the constants K_1 to K_6 are

defined as:

$$K_1 = \frac{X_q - X_d^{'}}{X_e + X_d^{'}} I_{q0} V_\infty sin\delta_0 + \frac{V_{q0} V_\infty cos\delta_0}{X_e + X_q}$$

$$K_2 = \frac{V_\infty}{X_e + X_d^{'}} sin\delta_0$$

$$K_3 = \frac{X_d^{'} + X_e}{X_d + X_e}$$

$$K_4 = \frac{X_d - X_d^{'}}{X_e + X_d^{'}} V_\infty sin\delta_0$$

$$K_5 = \frac{X_q}{X_e + X_q} \frac{e_{do}}{e_{to}} V_\infty cos\delta_0 - \frac{X_d^{'}}{X_e + X_d^{'}} \frac{e_{qo}}{e_{to}} V_\infty sin\delta_0$$

$$K_6 = \frac{X_e}{X_e + X_d^{'}} \frac{e_{q0}}{e_{to}}$$

where

P, Q	Active and reactive powers (p.u.)
D	Damping coefficient
H	Inertia constant (s)
ω	Rotor angular speed (rad/s)
ω_s	Synchronous rotor angular speed (rad/s)
δ	Power angle (rad)
δ_0	Initial Power angle (rad)
θ	Power angle (deg)
I_g	Generator current (p.u.)
I_d, I_q	d and q-axis components (p.u.) of the generator current
V_d, V_q	d and q-axis components (p.u.) of the generator voltage
K_A	AVR gain (p.u.)
T_A	AVR time constant (s)
R_e, X_e	Resistance and reactance of the transmission line (p.u.)
E_{fd}	Rotor field voltage (p.u.)
V_t	Terminal voltage (p.u.)
e_t	Initial terminal voltage (p.u.)
e_{d0}	Initial d-axis terminal voltage (p.u.)
e_{q0}	Initial q-axis terminal voltage (p.u.)
V_{ref}	Reference voltage (p.u.)
V_∞	Infinite bus voltage (p.u.)
T_m	Mechanical torque (p.u.)
T_e	Electrical torque (p.u.)
$E_q^{'}$	q-axis transient internal voltage (p.u.)
$T_{do}^{'}$	d-axis transient open circuit generator time constant (s)
X_d, X_q	generator d and q axis reactances (p.u.)
$X_d^{'}$	generator d-axis transient reactance (p.u.)

B. The SMIB Data

The numerical values of the SMIB parameters presented in Fig.1 are:

X_d	$X_d^{'}$	X_q	$T_{do}^{'}$	V_∞	H	ω_s	K_A	T_A
2.0	0.244	1.91	4.18	1.0	3.25	314.15	50.0	0.05
p.u	p.u	p.u	s	p.u	s	rad/s	p.u	s

C. The Convention power system stabilizer

The transfer function of the conventional power system stabilizer used in this paper is given as follows:

$$K_0(s) = K_s \frac{(s + T_1)^2}{(s + T_2)^2} \tag{16}$$

The conventional CPSS tuning parameters are obtained from [19].

REFERENCES

[1] P. Kundur, N. J. Balu, and M. G. Lauby, *Power system stability and control*. McGraw-hill New York, 1994, vol. 7.

[2] A. A. Sallam and O. P. Malik, *Power System Stability: Modelling, analysis and control*. Institution of Engineering and Technology, 2015.

[3] "IEEE Recommended Practice for Excitation System Models for Power System Stability Studies," *IEEE Std 421.5-2016 (Revision of IEEE Std 421.5-2005)*, pp. 1–207, Aug. 2016.

[4] K. Sreedivya, P. A. Jeyanthy, and D. Devaraj, "Design of power system stabilizer using sliding mode control technique for low frequency oscillations damping," in *2019 IEEE International Conference on Intelligent Techniques in Control, Optimization and Signal Processing (INCOS)*. IEEE, 2019, pp. 1–6.

[5] K. Kumara and A. Srinaivasan, "Design of pole placement power system stabilizer for SMIB-effect of operating conditions," in *2017 International Conference on Electrical, Electronics, Communication, Computer, and Optimization Techniques (ICEECCOT)*. IEEE, 2017, pp. 518–523.

[6] A. Sabo, N. I. Abdul Wahab, M. L. Othman, M. Z. A. Mohd Jaffar, and H. Beiranvand, "Optimal design of power system stabilizer for multimachine power system using farmland fertility algorithm," *International Transactions on Electrical Energy Systems*, p. e12657, 2020.

[7] M. Dubey, "Design of genetic algorithm based fuzzy logic power system stabilizers in multimachine power system," in *2008 Joint International Conference on Power System Technology and IEEE Power India Conference*. IEEE, 2008, pp. 1–6.

[8] D. Wang, N. Ma, M. Wei, and Y. Liu, "Parameters tuning of power system stabilizer PSS4B using hybrid particle swarm optimization algorithm," *International Transactions on Electrical Energy Systems*, vol. 28, no. 9, p. e2598, 2018.

[9] E. L. Miotto, P. B. de Araujo, E. de Vargas Fortes, B. R. Gamino, and L. F. B. Martins, "Coordinated tuning of the parameters of PSS and POD controllers using bioinspired algorithms," *IEEE Transactions on Industry Applications*, vol. 54, no. 4, pp. 3845–3857, 2018.

[10] G. Zhang, W. Hu, D. Cao, Q. Huang, J. Yi, Z. Chen, and F. Blaabjerg, "Deep reinforcement learning based approach for proportional resonance power system stabilizer to prevent ultra-low-frequency oscillations," *IEEE Transactions on Smart Grid*, 2020.

[11] S. Kamalasadan, G. D. Swann, and R. Yousefian, "A novel system-centric intelligent adaptive control architecture for power system stabilizer based on adaptive neural networks," *IEEE Systems Journal*, vol. 8, no. 4, pp. 1074–1085, 2013.

[12] M. Ramirez-Gonzalez and O. Malik, "Simplified fuzzy logic controller and its application as a power system stabilizer," in *2009 15th International Conference on Intelligent System Applications to Power Systems*. IEEE, 2009, pp. 1–6.

[13] K. Niimi, K. Yukita, T. Matsumura, and Y. Goto, "Verification of load frequency control using H_∞ control," in *2018 7th International Conference on Renewable Energy Research and Applications (ICRERA)*. IEEE, 2018, pp. 1174–1178.

[14] A. Sil, T. Gangopadhyay, S. Paul, and A. Maitra, "Design of robust power system stabilizer using H_∞ mixed sensitivity technique," in *2009 International Conference on Power Systems*. IEEE, 2009, pp. 1–4.

[15] S. Barik and A. T. Mathew, "Design and comparison of power system stabilizer by conventional and robust H_∞ loop shaping technique," in *2014 International Conference on Circuits, Power and Computing Technologies [ICCPCT-2014]*. IEEE, 2014, pp. 124–129.

[16] P. S. Rao and I. Sen, "Robust pole placement stabilizer design using linear matrix inequalities," *IEEE Transactions on Power Systems*, vol. 15, no. 1, pp. 313–319, 2000.

[17] P. Sauer, M. Pai, and J. Chow, *Power System Dynamics and Stability: With Synchrophasor Measurement and Power System Toolbox*. Wiley, 2017.

[18] F. P. Demello and C. Concordia, "Concepts of synchronous machine stability as affected by excitation control," *IEEE Transactions on power apparatus and systems*, vol. 88, no. 4, pp. 316–329, 1969.

[19] P. S. Rao and I. Sen, "Robust tuning of power system stabilizers using QFT," *IEEE transactions on control systems technology*, vol. 7, no. 4, pp. 478–486, 1999.